Supporting Information

Bottom-up fabrication of triazine-based frameworks as metal-free materials for supercapacitors and oxygen reduction reaction

Ronghan Cao,[a] Fangyuan Hu,[b,*] Tianpeng Zhang,[b] Wenlong Shao,[b] Siyang Liu,[b] Xigao Jian[a,b,c,*]

[a] *State Key Laboratory of Fine Chemicals, Department of Polymer Materials & Engineering，Liaoning Province Engineering Research Centre of High Performance Resins. Dalian University of Technology, Dalian, 116024, China.*

[b] *School of Materials Science and Engineering, Key Laboratory of Energy Materials and Devices (Liaoning Province), State Key Laboratory of Fine Chemicals, Liaoning Province Engineering Centre of High Performance Resins. Dalian University of Technology, Dalian 116024, China.*

** Corresponding Authors. E-mail: hufangyuan@dlut.edu.cn (F. Y. Hu), jian4616@dlut.edu.cn (X. Jian).*

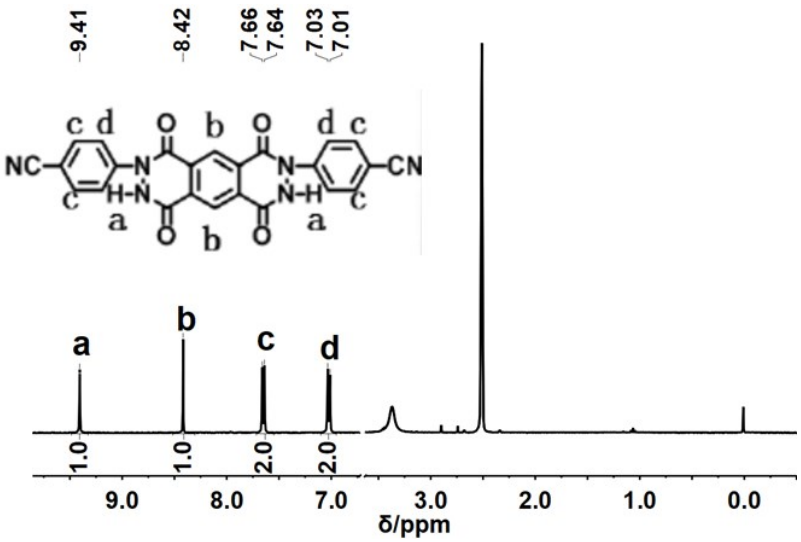

Fig. S1. ^{1}H-NMR spectrum of PYPZ (in DMSO-d^{6}).

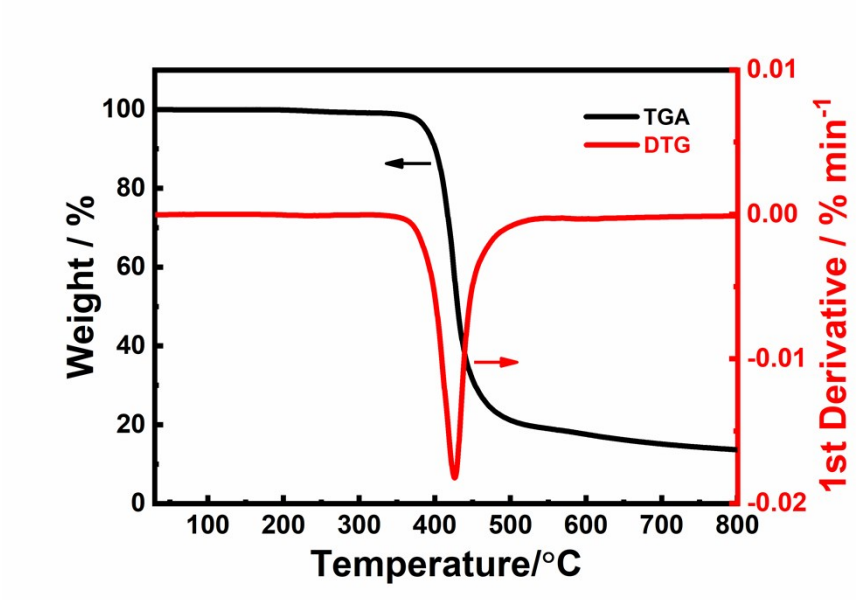

Fig. S2. The TGA and DTG curves of PYPZ monomer.

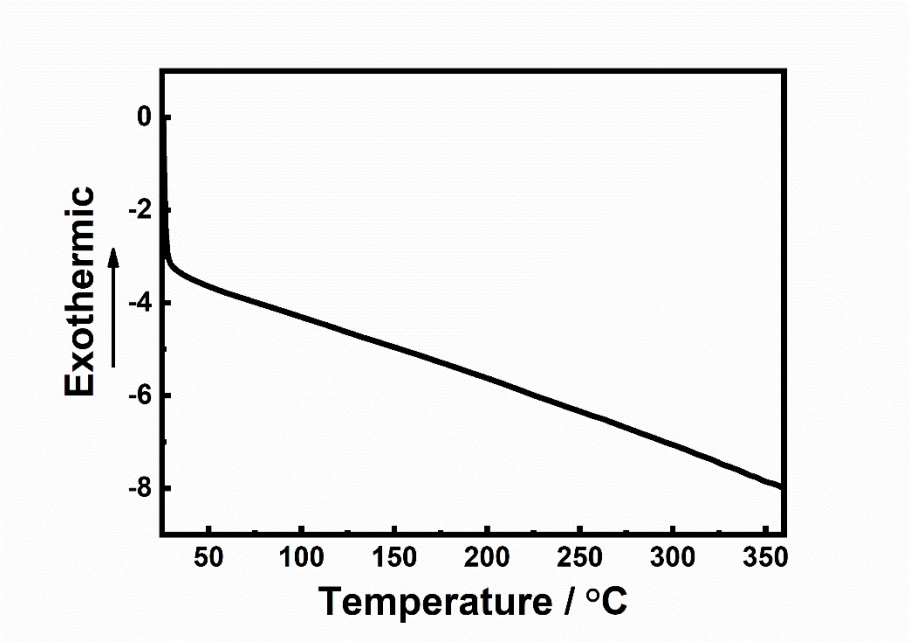

Fig. S3. The DSC curves of PYPZ monomer.

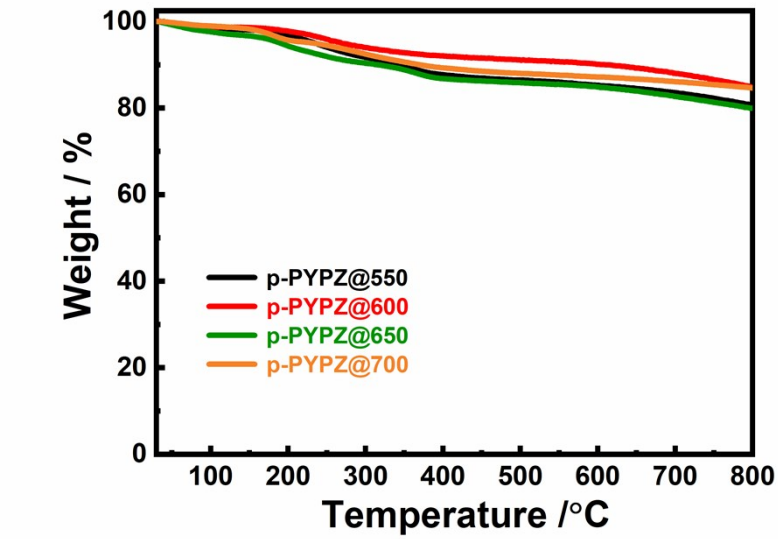

Fig. S4. The TGA spectra of p-PYPZs.

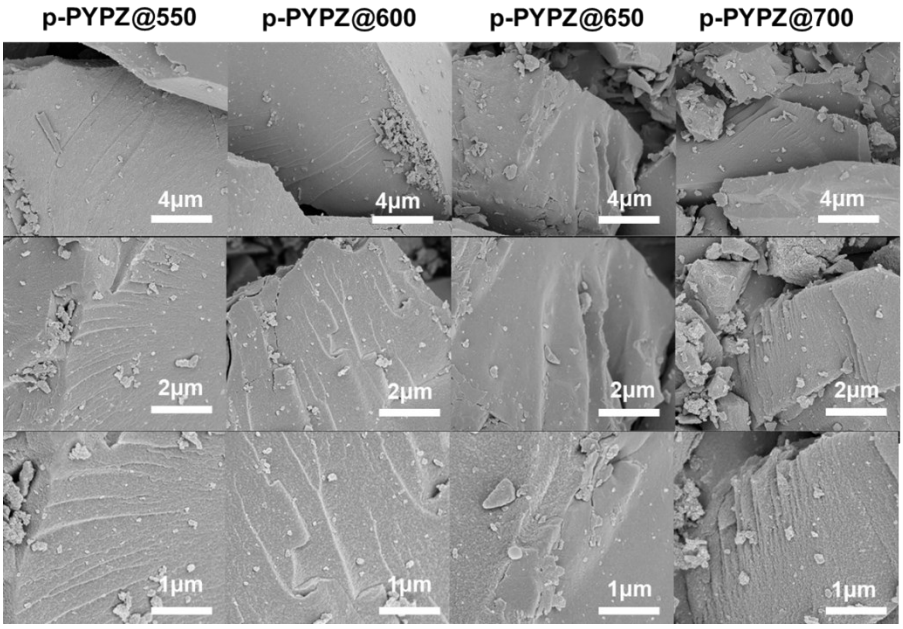

Fig. S5. SEM images of p-PYPZ@550, p-PYPZ@600, p-PYPZ@650, and p-PYPZ @700 at 1 μm, 2 μm, and 4 μm, respectively.

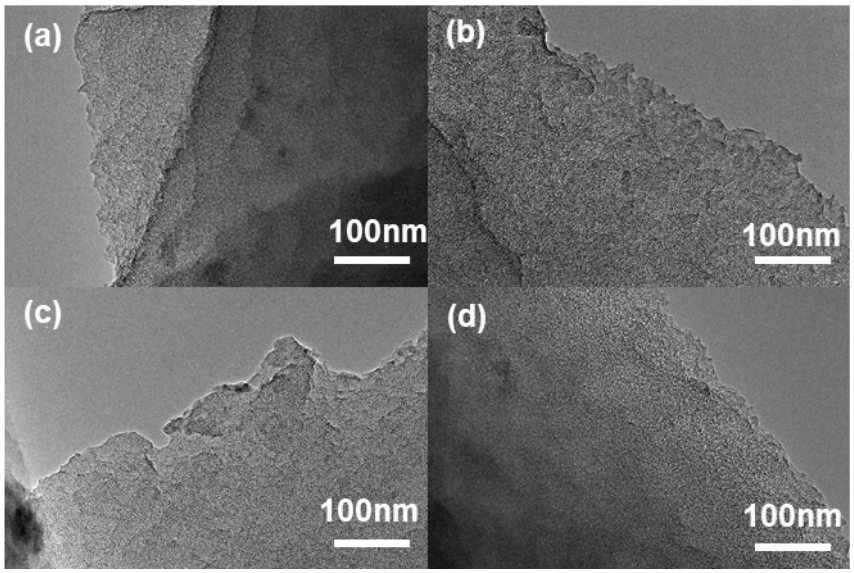

Fig. S6. TEM images of p-PYPZ@550, p-PYPZ@600, p-PYPZ@650, and p-PYPZ @700, respectively.

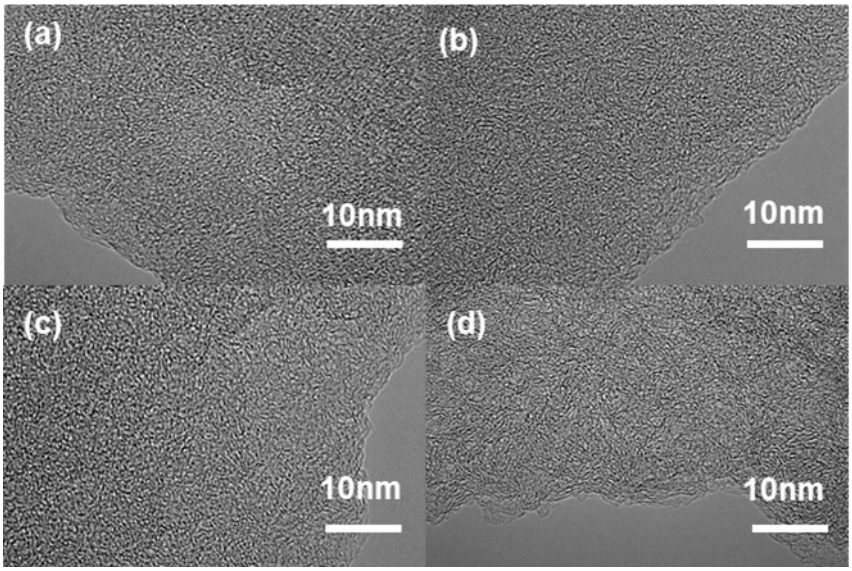

Fig. S7. HR-TEM images of p-PYPZ@550, p-PYPZ@600, p-PYPZ@650, and PYPZ @700, respectively.

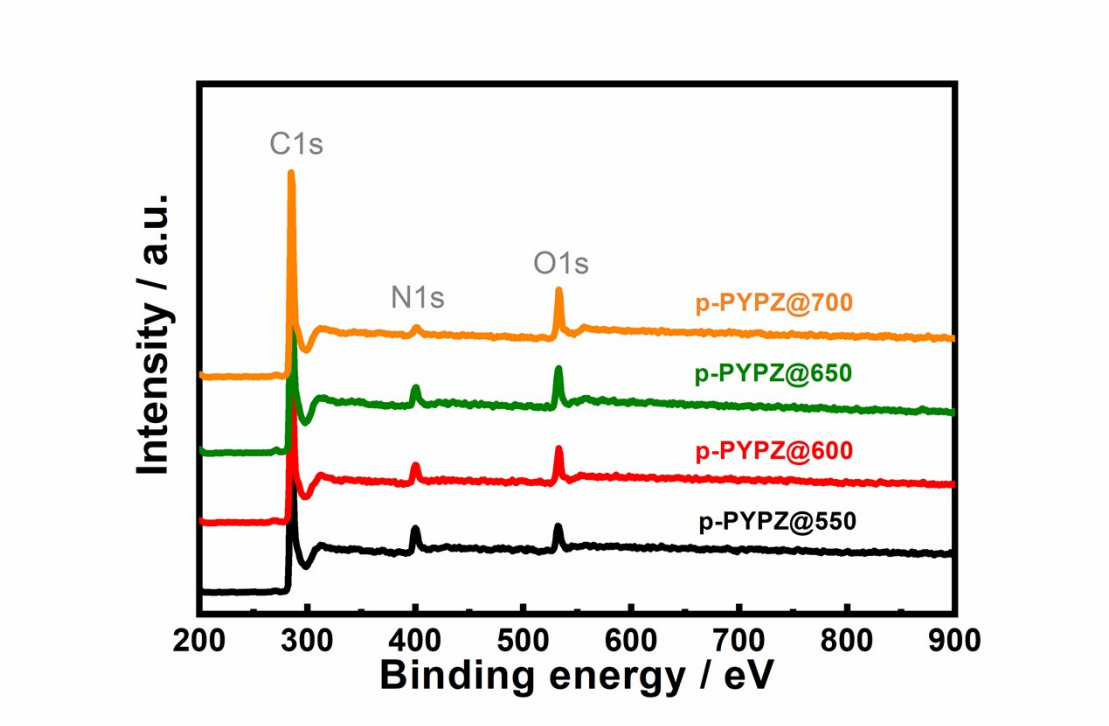

Fig. S8. XPS overall scanned spectrum of p-PYPZs

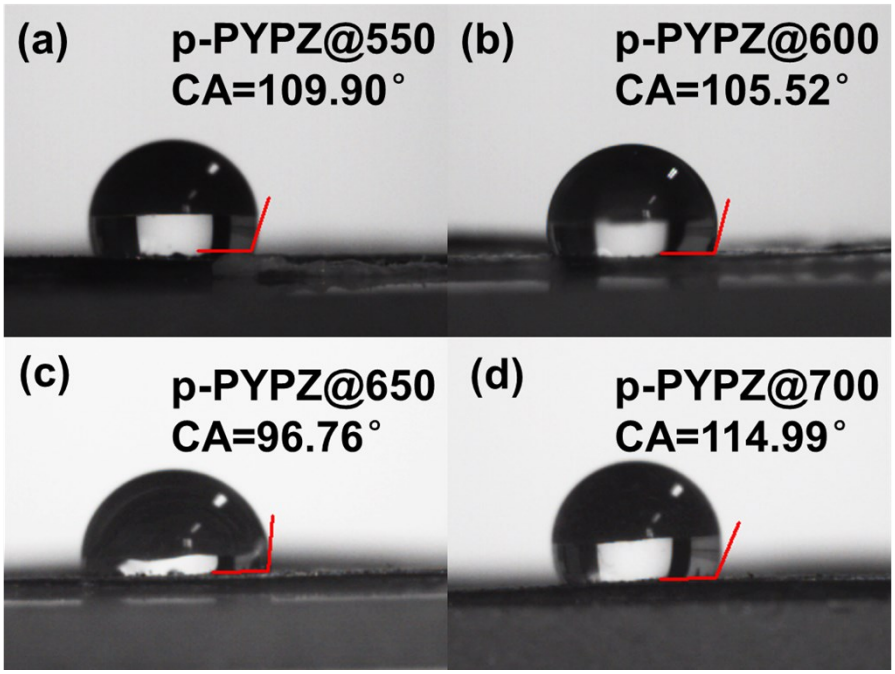

Fig. S9. Wetting angles of deionized water droplet on p-PYPZ@550, p-PYPZ@600, p-PYPZ@650, and PYPZ @700, respectively.

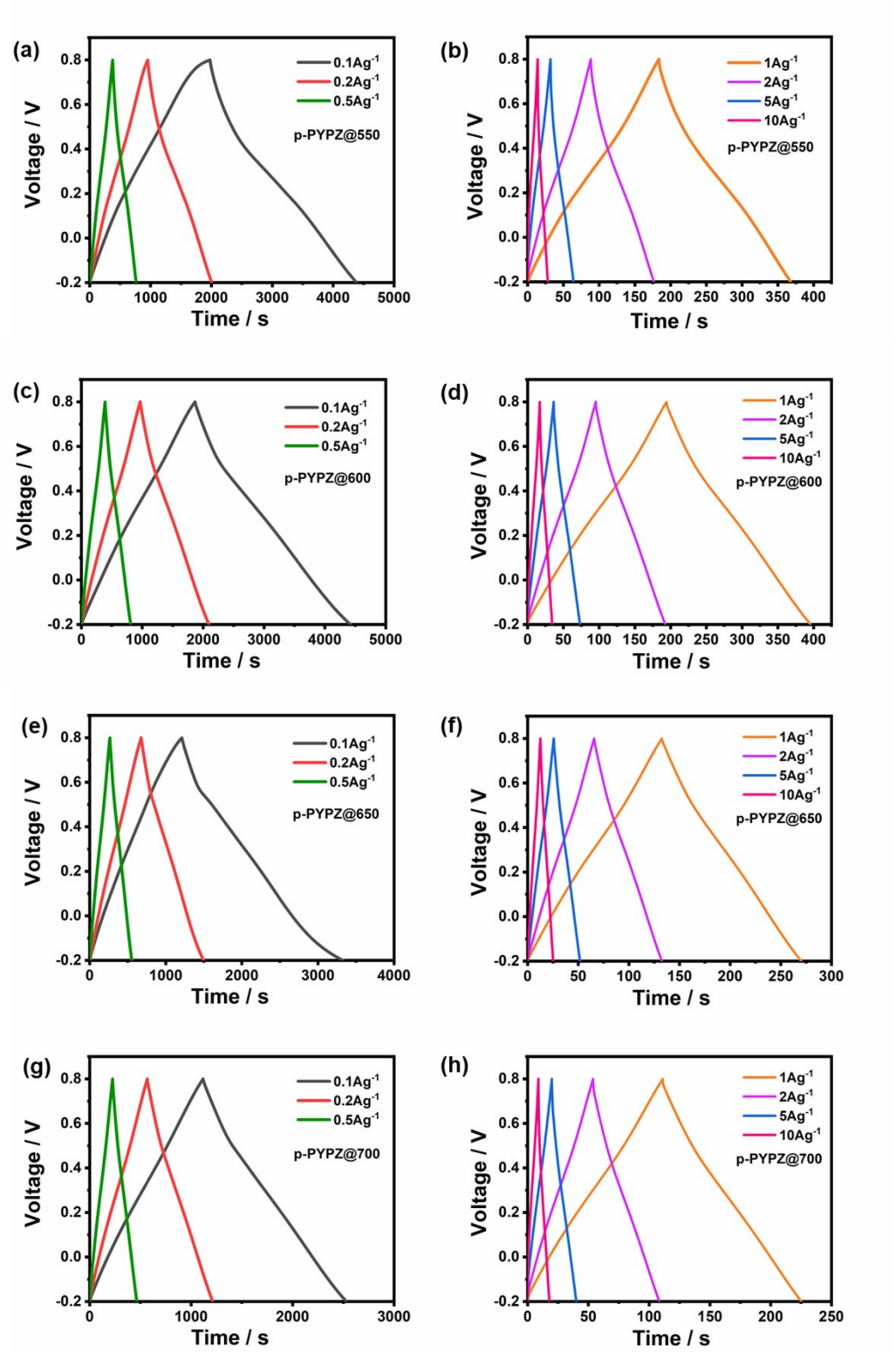

Fig. S10. The GC curves of p-PYPZS at various current densities in 1 M H_2SO_4: (a-b) GC measurements of p-PYPZ@550 at 0.1-10 A g^{-1}; (c-d) GC measurements of p-PYPZ@600 at 0.1-10 A g^{-1}; (e-f) GC measurements of p-PYPZ@650 at 0.1-10 A g^{-1}; (g-h) GC measurements of p-PYPZ@700 at 0.1-10 A g^{-1}.

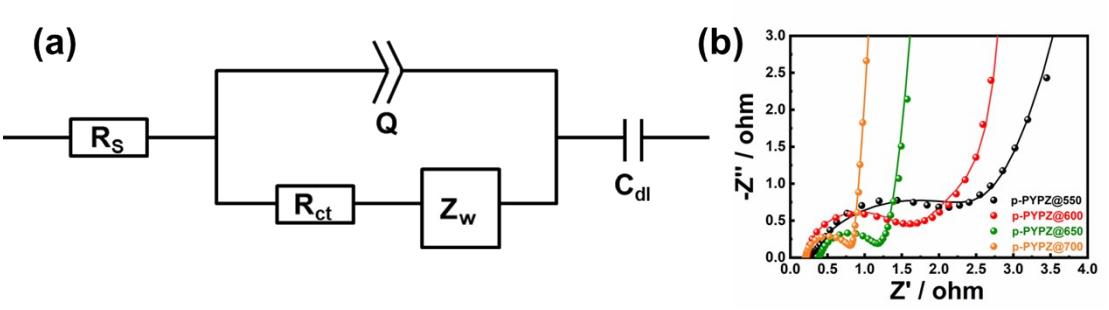

Fig. S11. (a) Equivalent circuit for the impedance spectra; (b) the equivalent circuit and the fitted data of EIS data of the p-PYPZs. (Points for experimental original data, and lines for fitting data)

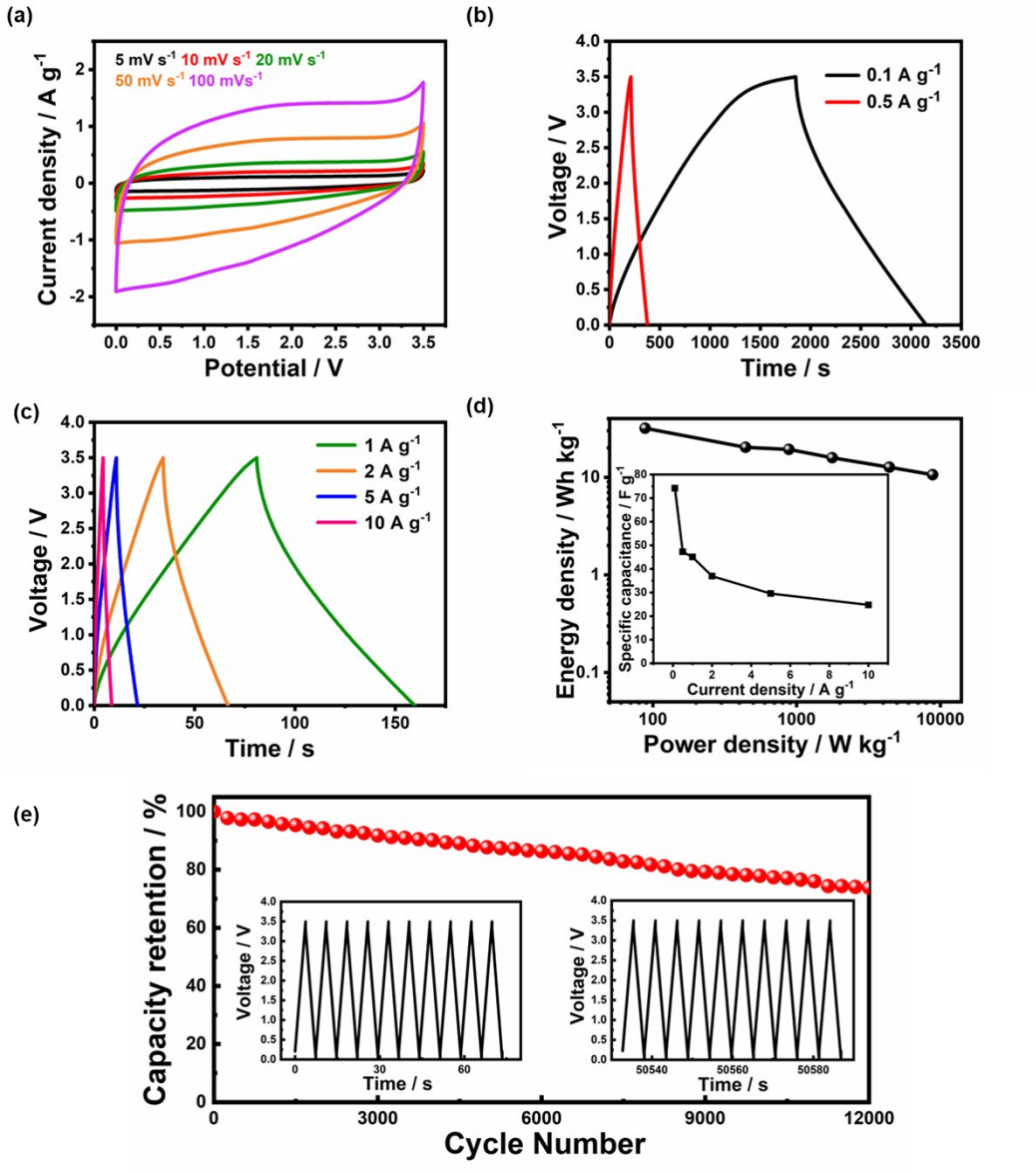

Fig. S12. (a) The CV curves of p-PYPZ@600 in [BMIM][BF_4]; (b,c)The GC curves of p-PYPZ@600 at various current densities in [BMIM][BF_4]; (d) Ragone plots (inset: specific capacitance at different current densities); (e) Long-term cycling tests of p-PYPZ@600 electrode with the electrolyte of [BMIM][BF_4] (inset: GCD curves for the first and last 10 cycles).

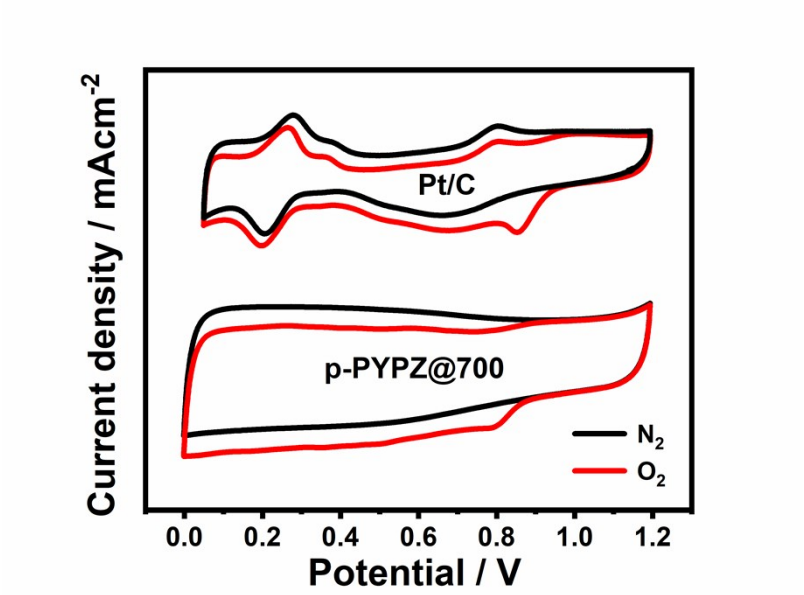

Fig. S13. The CV curves of Pt/C and p-PYPZ@700 in N_2 and O_2 saturated 0.1M KOH solution.

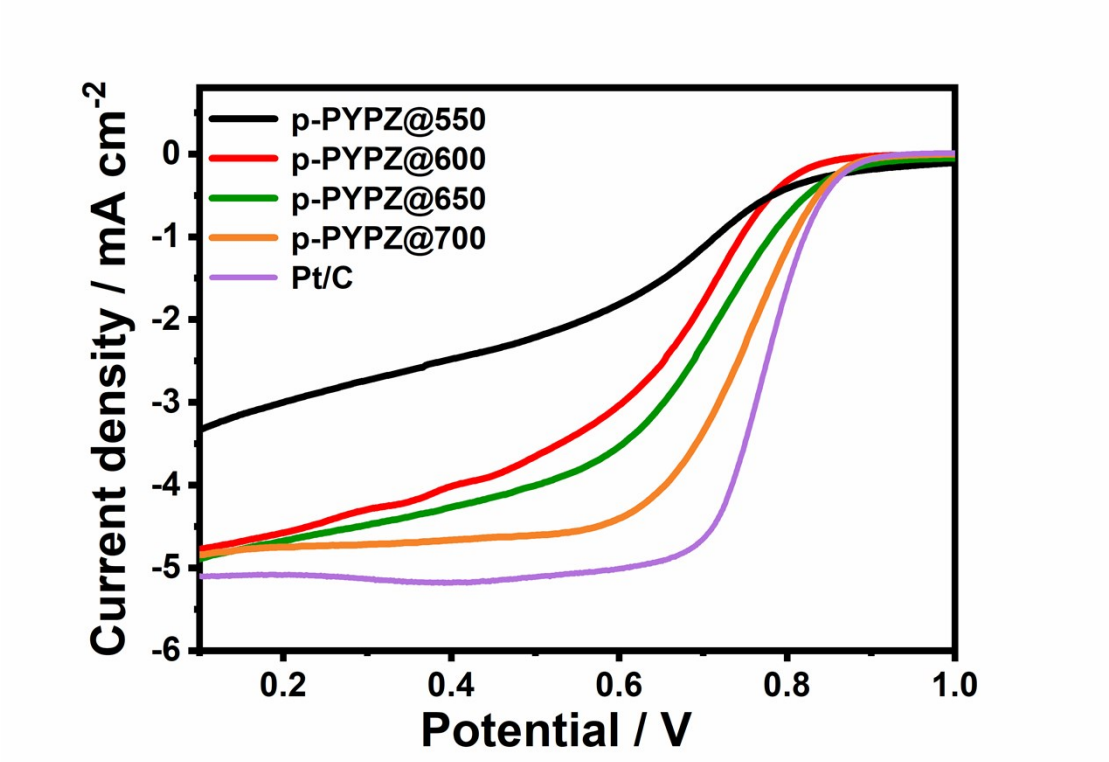

Fig. S14. The LSV curves of p-PYPZs and Pt/C.

Tab. S1. Atomic carbon, hydrogen and nitrogen contents of PYPZ based on elemental analysis.

	C (wt.%)	H (wt.%)	N (wt.%)
Theoretical value	64.29	2.70	18.74
Measured value	64.13	2.73	18.78
Relative error	0.16	0.03	0.04

Tab. S2. Element content analyzed via XPS and EA

Samples	XPS		EA
	N (at.%)	O (at.%)	N (wt.%)
p-PYPZ@550	8.10	5.23	8.85
p-PYPZ@600	6.48	5.92	6.82
p-PYPZ@650	5.54	6.98	5.21
p-PYPZ@700	3.46	5.18	3.50

Tab. S3. Relative content of N species obtained from the deconvolution analysis results of N1s core level XPS spectra

Samples	N-5[b] (%)	N-6[c] (%)	N-Q[d] (%)
p-PYPZ@550[a]	15.01	38.04	46.95
p-PYPZ@600[a]	19.07	28.92	52.01
p-PYPZ@650[a]	12.37	34.98	52.65
p-PYPZ@700[a]	8.59	23.97	67.44

[a] Relative intensity, data from XPS curves; [b] 399.7 eV from N1s XPS curves; [c] 398.0 eV from N1s XPS curves;

Tab. S4. Pore structures parameters of p-PYPZs

Samples	S_{BET}[a] ($m^2\ g^{-1}$)	V_t[b] ($cm^3\ g^{-1}$)	L[c] nm
p-TIDN@550	981.6	0.65	0.79
p-TIDN@600	999.4	0.71	0.85
p-TIDN@650	1242	0.73	0.82
p-TIDN@700	1464	0.93	0.82

[a] Specific surface area of p-PYPZs is calculated by BET method in N_2 (77K). [b] Total pore volume was determined at the relative pressure of 0.99. [c] Average pore sizes of p-PYPZs.

Tab. S5 Comparison of the p-PYPZ@600 electrode with reported heteroatom-doped carbon electrodes in terms of cycle performance

Sample	Heteroatoms	S_{BET} (m^2 g^{-1})	Specific capacitance	Retention (cycles)	Electrolyte
p-PYPZ@600	N 6.48 at.%, O 5.92 at.%	999	256 F g^{-1} at 0.1 A g^{-1}	110%(35000)	1 M H_2SO_4
NMC-4[1]	N 5.69 at.%	995	178.5 F g^{-1} at 0.5 A g^{-1}	94.5%(5000)	6 M KOH
HN-CMs[2]	N 19.22 wt.%	323	266.7 F g^{-1} at 5 mV s^{-1}	94.7%(5000)	1M KOH
BN-Gas[3]	N 0.6 at.%, B 3.0 at.%	249	239 F g^{-1} at 1 mV s^{-1}	100%(1000)	1 M H_2SO_4
NHPC-0.5[4]	N 12.1 at.%	1798	283.7 F g^{-1} at 1 A g^{-1}	105.8%(40000)	1 M H_2SO_4
Glu-$(NH_4)_3PO_4$-800[5]	N 4.8 wt.%, P 2.1 at.%, O 8.4 at.%	445	184 F g^{-1} at 0.05 A g^{-1}	>90%(2000)	6 M KOH
f-MHCFs@600[6]	N 6.83 wt.%, P 2.25 at.%, O 6.22 at.%, F 7.23 at.%	994	244.8 F g^{-1} at 0.1 A g^{-1}	98.5%(10000)	1 M H_2SO_4
N1-GDY[7]	N 3.67 at.%	679	247 F g^{-1} at 0.1 A g^{-1}	95.6%(3000)	7 M KOH
HP-CF[8]	N 18.7%	1175	222.0 at 2 mV s^{-1}	91.2%(10000)	3 M KOH
CNB-3[9]	N 0.5 wt%, B 0.7 wt%	376	247 at 0.5 A g^{-1}	96.2% (4000)	6 M KOH

References

[1] G. Lin, R. Ma, Y. Zhou, C. Hu, M. Yang, Q. Liu, S. Kaskel, J. Wang, J. Colloid Interface Sci. 527 (2018) 230-240.
[2] M. Hassan, D. Wu, X. Song, W. Qiu, Q. Mao, S. Ren, C. Hao, Journal of Electroanalytical Chemistry 829 (2018) 157-167.
[3] Z.S. Wu, A. Winter, L. Chen, Y. Sun, A. Turchanin, X. Feng, K. Mullen, Adv. Mater. 24 (2012) 5130-5.
[4] H. Sun, H. Quan, M. Pan, Z. Zhang, Y. Zeng, D. Chen, Journal of Alloys and Compounds 826 (2020).
[5] C. Wang, Y. Zhou, L. Sun, P. Wan, X. Zhang, J. Qiu, J. Power Sources 239 (2013) 81-88.
[6] F. Hu, T. Zhang, J. Wang, C. Liu, S. Li, S. Hu, X. Jian, ACS Sustainable Chemistry & Engineering 6 (2018) 15764-15772.
[7] H. Shang, Z. Zuo, H. Zheng, K. Li, Z. Tu, Y. Yi, H. Liu, Y. Li, Y. Li, Nano Energy 44 (2018) 144-154.
[8] Z. Chen, K. Liu, S. Liu, L. Xia, J. Fu, X. Zhang, C. Zhang, B. Gao, Electrochimica Acta 237 (2017) 102-108.
[9] D.-C. Guo, J. Mi, G.-P. Hao, W. Dong, G. Xiong, W.-C. Li, A.-H. Lu, Energy Environ. Sci. 6 (2013) 652-659.